sensors

MDPI

Article

A statistical approach for functional reach-to-grasp segmentation using a single inertial measurement unit

Gregorio Dotti [1*], Marco Caruso [1], Daniele Fortunato [1], Marco Knaflitz [1], Andrea Cereatti [1], and Marco Ghislieri [1]

[1] PolitoBIOMed Lab and Department of Electronics and Telecommunications, Politecnico di Torino, 10129, Turin, Italy; Email: gregorio.dotti@polito.it (G.D.), marco.caruso@polito.it (M.C.), daniele.fortunato@polito.it (D.F.), marco.knaflitz@polito.it (M.K.), andrea.cereatti@polito.it (A.C.), marco.ghislieri@polito.it (M.G.).

* Correspondence: gregorio.dotti@polito.it

Abstract: The aim of this contribution is to present a segmentation method for the identification of voluntary movements from inertial data acquired through a single inertial measurement unit placed on the subject's wrist. Inertial data were recorded from 25 healthy subjects while performing 75 consecutive reach-to-grasp movements. The approach herein presented, called DynAMoS, is based on an adaptive thresholding step on the angular velocity norm, followed by a statistics-based post-processing on the movement duration distribution. Post-processing aims at reducing the number of erroneous transitions in the movement segmentation. We assessed the segmentation quality of this method using a stereophotogrammetric system as the gold standard. Two popular methods already presented in the literature were compared to DynAMoS in terms of the number of movements identified, onset and offset mean absolute errors, and movement duration. Moreover, we analyzed the sub-phase durations of the drinking movement to further characterize the task. Results showed that the proposed method performs significantly better than the two state-of-the-art approaches (i.e., percentage of erroneous movements = 3%; onset and offset mean absolute error < 0.08 s), suggesting that DynAMoS could make more effective home monitoring applications for assessing the motion improvements of patients following domicile rehabilitation protocols.

Keywords: Activity of daily living; functional assessment; IMU; movement segmentation; telerehabilitation; upper limb

Citation: To be added by editorial staff during production.

Academic Editor: Firstname Lastname

Received: date
Revised: date
Accepted: date
Published: date

1. Introduction

Activities of Daily Living (ADLs) are fundamental for independent living and, in this regard, the functionality of the upper limb is crucial for a good quality of life [1,2]. Unfortunately, 28% of the population over 50 years of age and 50% of the population over 80 years are affected by movement disorders [3].

To define appropriate interventions for motor disorders management, an accurate clinical assessment sets the basis for designing an effective motor rehabilitation program and for testing its effectiveness. Clinical assessment is usually performed using scales grading functional and movement disorders based on the clinician's evaluation of the execution of a specific task. However, in the last decades, many motion analysis systems have been proposed and used for reducing the subjectivity in patient clinical evaluation and enhancing the effectiveness of rehabilitation outcome evaluation, especially for the upper limb [4–8]. In particular, Inertial Measurement Units (IMUs) have been widely used for the assessment and rehabilitation of movement disorders of the upper limb [9]. IMUs measure acceleration and angular velocity of the body segment they are fixed to, allowing for the quantitative analysis of patient movements based on parameters derived from inertial recordings [9]. The use of IMUs arose because of their ease of use, portability, and low cost. For example, using IMUs allows clinicians to tailor rehabilitation protocols to the patient's needs [10] and, in the context of therapy delivery systems, allows patients to decide when and where to carry out therapeutic sessions [11]. However, these devices are not yet considered adequate for measuring the quality of movement during functional tasks in a clinical environment [12]. Therefore, there is a need to develop and validate new methods that increase the reliability and validity of IMU-derived evaluation metrics in clinics [12].

Among all the proposed parameters, execution time is one of the most commonly used metrics for the assessment of patient functionality in a clinical context. Hence, it is necessary to precisely identify voluntary movements. To this end, several methods, based on the inertial data, have been presented in the literature. The most straightforward approach is to define a threshold that discriminates between voluntary movements and involuntary ones. For example, Schwarz *et al.* [13] identified voluntary movements by applying a fixed threshold to the angular velocity norm. Voluntary movements were identified in correspondence to the time instants above this threshold. Carpinella *et al.* [14] proposed a similar approach setting an adaptive threshold at 25% of the maximum of the angular velocity norm during the movement. Setting the threshold value equal to a percentage of the maximum recorded value guarantees that the threshold is more suited to the characteristics of the subject under analysis, reducing the influence of inter-subject variability on the segmentation results. Moreover, Hughes *et al.* [15] identified voluntary movement onset and offset by applying a kinematic criterion on the linear velocity derived from the IMU accelerometer. In detail, the onset was determined as the first instance in the time series where the resultant velocity exceeded 1.5% of the first velocity peak, and the offset was determined when the velocity dropped under 1.5% of the velocity peak. The method proposed by Hughes *et al.* presents several challenges. First, the reconstruction of the linear velocity relies on numerically integrating the linear acceleration after removing the gravitational bias. This process requires accurately estimating the sensor orientation using a sensor fusion filter. Even with fine-tuning of the filter parameters residual errors persist, leading to propagation errors in the numerical integration process [16]. Additionally, the initial conditions of orientation and velocity are critical factors that significantly impact the accuracy of the results. Repnik *et al.* [17] presented a different segmentation method, based on the biomechanical model reconstruction of the upper limb from multiple IMUs mounted on the patient chest, arm, and forearm. Apart from the approach used by Schwarz *et al.* [13], all the other methods cannot be used in real-time applications since they need to extract information from the whole IMU recordings before performing movement segmentation.

Among the aforementioned methods, the most used approaches for voluntary movement segmentation are those presented by Schwarz *et al.* [13] and Carpinella *et al.* [14], due to their simplicity and scalability. Nevertheless, both methods are subject to limitations. The segmentation method proposed by Schwarz *et al.* [13] does not present a technical validation. Moreover, the application of a fixed arbitrary threshold may strongly reduce the adaptability of the method to different movement and subject characteristics. These limitations have been partially solved by Carpinella *et al.* [14], who performed a technical validation and employed an adaptive threshold to identify voluntary movement from the angular velocity norm. However, the definition of the adaptive threshold can have a significant impact on the final segmentation results. The choice of a high value (e.g., 25% of the maximum angular velocity norm) could lead to the exclusion of parts of movements or even whole movements. On the other hand, selecting a value that is too low may lead to the inclusion of involuntary movements or background noise. This is especially true when analyzing movements that are composed of sub-phases executed at very different intensity levels. Moreover, the reliability of the segmentation results may be compromised by signal fluctuations around the threshold value, resulting in fast erroneous transitions.

To overcome the limitations of the approaches proposed by Schwarz *et al.* [13] and Carpinella *et al.* [14], we developed a new method and performed a technical validation using a StereoPhotogrammetric (SP) system as a gold standard. The newly proposed segmentation method, DynAMoS (Dynamic Adaptive Movement Segmentation), enhances the state-of-the-art adaptive thresholding approach with statistics-based post-processing aimed to reduce erroneous segmentation by applying statistical considerations to the movement duration histograms. In this paper, after the evaluation of the effectiveness of the proposed method against the gold standard and state-of-the-art approaches (i.e., Schwarz *et al.* [13] and Carpinella *et al.* [14]), segmentation results are used for the characterization of a reach-to-grasp movement. With the aim of supporting the adoption and standardization of IMU-derived parameters in clinical environment, we freely distribute the DynAMoS Matlab algorithm, its detailed documentation, and a sample dataset on the BIOLAB GitHub repository (https://github.com/Biolab-PoliTO/DynAMoS).

2. Materials and Methods

2.1 Participants

Twenty-five healthy subjects (12 females and 13 males; age: 22.5 ± 2.1 years; 6 left-handed and 19 right-handed) participated in the study. To participate, volunteers were required to have no history of physical or neurological pathologies that might interfere with their ability to perform the task. The subject height and weight were recorded by self-report. The dominant forearm length was measured with a flexible measuring tape with the forearm facing downward, measuring from the lateral epicondyle to the ulnar styloid process.

This study was approved by the Ethics Committee of Politecnico di Torino (Protocol N. 24766/2022, approved on July 19, 2022). Written informed consent was obtained from each participant before the experimental sessions, and all the acquisitions were performed following the Declaration of Helsinki.

2.2 Acquisition System

Recordings were carried out at the Motion Analysis Laboratory of Polito^{BIO}Med Lab, Politecnico di Torino (Turin, Italy). Inertial data were recorded using an IMU-based wearable device designed and developed at the BIOLAB of Politecnico di Torino (Turin, Italy). This device incorporates an IMU featuring a three-axial accelerometer and gyroscope (LSM9DS1, STMicroelectronics), a Bluetooth Low Energy module, a floating-point microcontroller (SAME70, Microchip) to easily install and run custom algorithms onboard, a micro-SD card to store raw and processed data, and an 1 Ah rechargeable battery [18]. All the IMU recordings are acquired at a sampling frequency of 100 Hz.

A twelve infrared camera SP system (Vicon T20, Vicon Motion Systems, sampling frequency: 100 Hz) was used to reconstruct the trajectories of 4 photo-reflective markers (diameter: 9.5 mm) attached to the IMU. The IMU was secured to the wrist of the subject using double-sided adhesive tape [19] with its short edge roughly aligned with the wrist's flexion-extension axis.

Three RGB cameras integrated with the SP system were used to record the acquisitions (sampling frequency: 50 Hz). Video recordings were anonymized by blurring subjects' faces.

Figure 1a shows a schematic representation of the acquisition system.

The IMU and SP signals were then imported into MATLAB release r2023b (The MathWorks Inc., Natick, MA, USA) to be offline processed through custom routines.

2.3 Experimental Protocol

Volunteers were seated at a table (distance between the tabletop and the seat: 30 cm; table height: 70 cm) and were asked to perform a drinking task using their dominant upper limb. The bottle was positioned in front of the subject sternum at a distance from the table edge equal to 1.5 times the forearm length. The drinking task consisted of reaching

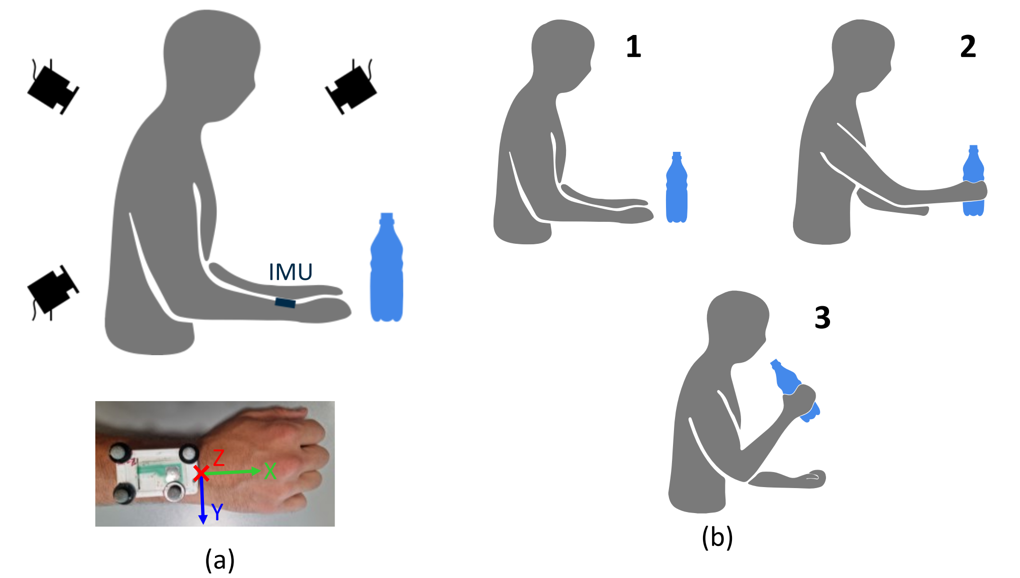

Figure 1. Panel (a): Representation of the acquisition setup composed by the SP system and the IMU (in dark blue color) and a picture of the wrist-worn IMU with 4 photo-reflective markers. Panel (b): Representation of the drinking task sub-phases. The drinking task consisted of reaching and grasping the bottle (step 1 and 2), lifting the bottle simulating drinking (step 2 and 3), placing the bottle back on the table (step 3 and 2), and returning to the resting position (step 2 and 1).

and grasping the bottle (Phase I), lifting the bottle simulating drinking (Phase II), placing the bottle back on the table (Phase III), and returning to the resting position (Phase IV). **Figure 1b** schematically represents the experimental protocol with the indication of the three task sub-phases. The investigated task represents a typical ADL and is part of the Frenchay Arm Test, which is commonly used to evaluate upper limb function [20]. The position of the bottle on the table and the wrist resting position were marked using adhesive tape, to ensure the repeatability of the movement.

At the start of each trial, subjects were requested to perform a 30-second static acquisition, after which they were instructed to raise the instrumented arm (dominant side) and perform three rapid rotations along the forearm longitudinal axis before returning to the resting position for 30 seconds. This movement was necessary to synchronize the SP system and the wrist-worn IMU. Subsequently, subjects were required to perform 25 repetitions of the drinking task. The drinking task sub-phases were executed following verbal instructions from the investigator. Between consecutive drinking tasks belonging to the same trial, a resting period of 4 seconds was performed. In conclusion, a single trial consisted of a 30-second static acquisition, a synchronization movement, another 30-second static acquisition, and 25 consecutive repetitions of the drinking task. Each volunteer completed three consecutive trials with a 2-minute rest in between. For each trial, considering the sub-phases as separated movements, 100 movements are expected.

2.4 Data Pre-Processing and Synchronization

The IMU position in space was reconstructed using the Vicon Nexus 2.12 software. The marker trajectories were visually checked and possible gaps were manually filled. To remove random noise, marker trajectories were low-pass filtered using a 2^{nd}-order zero-lag Butterworth filter with a cut-off frequency of 6 Hz. A Marker-cluster Local Frame (MLF) was defined using the markers attached to the IMU to determine its reference orientation with respect to the SP system global reference frame. The orientation of the MLF was performed using the Singular Value Decomposition (SVD) [21]. Then, the angular velocities were obtained from the orientation data [22]. The angular velocities estimated from the SP system were cross-correlated with the angular velocities recorded through the IMU to synchronize the two systems.

To reduce rapid signal fluctuations that could lead to inaccurate movement segmentation, marker trajectories and IMU recordings were further smoothed by means of a 4th-order zero-lag low-pass Butterworth filter with a cut-off frequency of 1.5 Hz.

2.5 Movement Segmentation

2.5.1 Stereophotogrammetric-based segmentation

Considering the SP system, voluntary movements were identified based on linear rather than angular velocity. Tri-axial linear velocity and its norm ($|v|$) were calculated from the marker trajectories. Each linear velocity norm was normalized in amplitude between 0 and 1 considering the absolute maximum value recorded over the task duration ($|v\_max|$). To determine voluntary movement onset and offset, an adaptive threshold was implemented, defined as the average over trials of the optimal thresholds computed through Otsu's method from the linear velocity norm of each trial [23,24]. Otsu's method is an unsupervised threshold selection method developed in image processing for the separation of objects from the background using the image gray-level histogram. In our case, Otsu's method was applied to the normalized linear velocity norm to identify the threshold that best distinguishes between the "background" (i.e., involuntary movements or background noise) and the "main object" (i.e., voluntary movements). Based on Otsu's method, the optimal threshold is selected as the one maximizing the inter-class variance. In this study, the adaptive threshold for the SP-based segmentation (Th_{SP}) was set equal to $0.11 \cdot |v\_max|$.

Additionally, the results of the SP-based segmentation were manually checked by an expert operator, using the videos of the acquisitions as a reference. These segmentations were considered the Gold Standard (GS) for the IMU-based segmentation approaches.

Figure 2a shows an example of voluntary movement segmentation obtained considering the SP-derived linear velocity norm.

2.5.2 IMU-based segmentation

The performance of the Dynamic Adaptive Movement Segmentation (DynAMoS) method was compared against two of the most widely used approaches: the fixed thresholding approach proposed by Schwartz *et al.* (M1) [13] and the adaptive thresholding approach proposed by Carpinella *et al.* (M2) [14]. All the tested methods were based on the application of a threshold on the angular velocity norm (Ω). In the following, the three tested segmentation approaches are described:

a) Fixed thresholding by Schwarz et al. (M1): The method consists of the application of a single threshold (Th_{M1}) whose value was set equal to $0.1\, rad/s$. Ω values higher than the threshold are identified as voluntary movements. This empirically selected threshold represents a reasonable value for discriminating between stationary and non-stationary states. **Figure 2b** represents the segmentation results obtained by applying the M1 method to the angular velocity norm of a representative healthy subject during a drinking task;

b) Adaptive thresholding by Carpinella et al. (M2): The method consists of the application of an adaptive threshold defined as $Th_{M2} = 0.25 \cdot \Omega_{max}$, where $\Omega_{\max}$ represents the maximum value of the angular velocity norm recorded over task duration. Setting the threshold to 25% of the maximum value of the angular velocity norm represents a more conservative approach to the segmentation task, ensuring that all the segmented sections are actual movements. **Figure 2c** represents the segmentation results obtained by applying the M2 method to the angular velocity norm of a representative healthy subject during a drinking task;

c) Dynamic Adaptive Movement Segmentation (DynAMoS): This newly proposed algorithm is based on an adaptive threshold and statistics-based post-processing applied to the duration of the identified movements to compensate for erroneous segmentations. The post-processing step implemented in DynAMoS was originally developed for clinical gait analysis to improve gait cycle segmentation [25]. First, movement onset and offset are identified through the application of an adaptive threshold to the angular velocity norm Ω. In particular, the adaptive threshold was defined as $Th_{DynAMoS} = 0.11\,\Omega_{max}$, where $\Omega_{\max}$ represents the maximum value of the angular velocity norm recorded during the task and the multiplicative constant was defined through Otsu's method [23,24] as detailed in section *2.5.1 Stereophotogrammetric-based segmentation*. Then, the duration of each segmented movement was calculated as the difference between the offset and onset time instants. Finally, the statistics-based post-processing is iteratively applied to the movement durations according to the following steps:

1. Definition of the movement duration histogram (see **Figure 3**) and computation of the median (M) value;
2. From the median value M, the lower threshold αM (with $0 < \alpha < 1$) and the upper threshold βM (with $1 < \beta < 2$) are obtained. The two thresholds will be used to identify data distribution outliers (i.e., movements characterized by "atypical" durations). The algorithm analyzes movements with "atypical" durations. If a movement has a duration lower than the threshold αM, the algorithm tries to merge it with the preceding or following movement. Meanwhile, if a movement has a duration longer than the upper threshold βM, the algorithm tries to split it into two movements. In the case of a duration lower than the threshold αM, the algorithm attempts to merge the movement under analysis with the preceding or the following, separately. The first attempt is performed with the merging candidate closest in time. If it fails, the other movement is considered. Merging fails if the new movement duration is lower than αM or higher than the βM thresholds. If none of the attempts satisfies the thresholds,

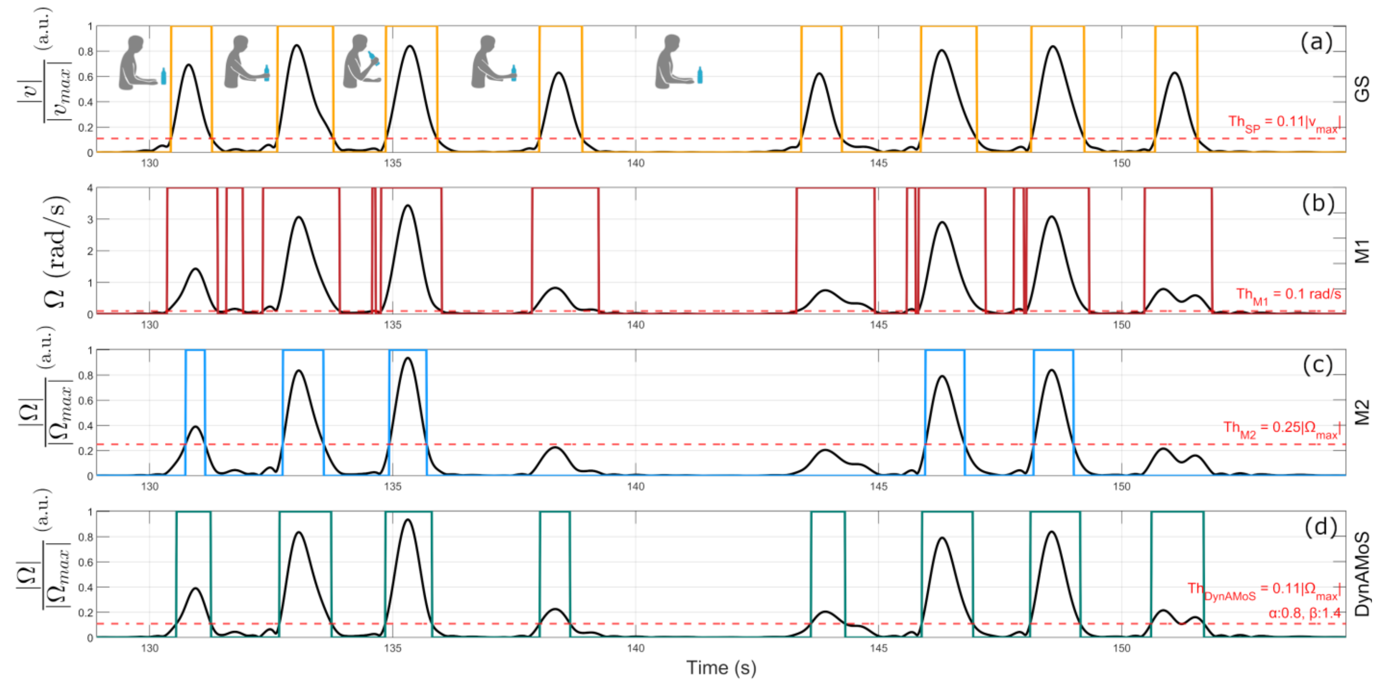

Figure 2. Example of segmentation results obtained through the application of the the gold standard and three tested methods (i.e., the method by Schwarz *et al.* – M1, the method by Carpinella *et al.* – M2, and the newly proposed method - DynAMoS) on inertial data acquired during drinking tasks. Dotted horizontal lines represent the threshold values of each method, while colored binary masks represent the segmentation output of each method.

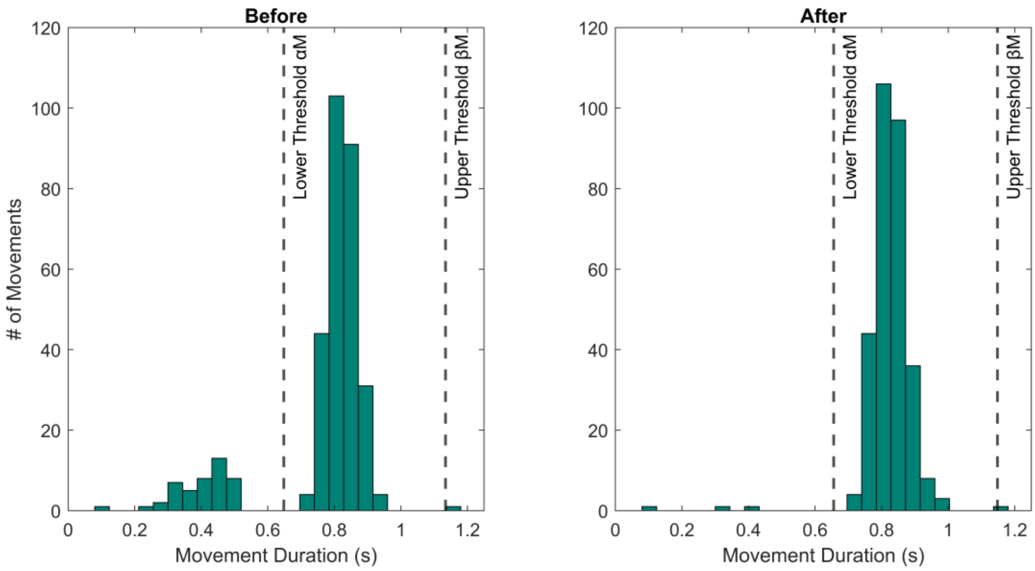

Figure 3. Example of movement duration histograms before (left side) and after (right side) the application of the statistics-based post-processing.

the movements are not merged. In case of merging success, the extremities of the "parent" movements are used as starting and ending points. In the case of a movement with a duration longer than the upper threshold βM, the algorithm tries to split it into two movements. To this purpose, the algorithms use local minima points in the signal as possible splitting points. From the minimum point with the lowest value, it splits the movement in two, with the new ending and new starting at the identified minimum. If these movements have a length longer than αM and shorter than βM thresholds, the split is accepted and the two new movements are created. Otherwise, the algorithm moves to another minimum point, if it exists;

3. After each splitting or merging event, M, αM, and βM values are updated considering the new movements;
4. The algorithm runs iteratively until all the movement duration outliers are processed.

Further details about DynAMoS functioning are freely available on the BIOLAB GitHub repository (https://github.com/Biolab-PoliTO/DynAMoS).

Figure 2d represents an example of segmentation obtained using the previously described method.

The optimization of the parameters α and β was performed using a grid search approach on all the acquired IMU data. Specifically, the value of α was chosen between 0.5 and 0.95 with steps of 0.05. Similarly, β was chosen between 1.05 and 1.5 with steps of 0.05. To find the best pair of parameters the following cost function (Fc) was defined as detailed in **Eq. (1)**:

$$F_c = \frac{Extra_{IMU}}{Total_{IMU}} + \frac{Missing_{IMU}}{Total_{IMU}} + \overline{\Delta Onset} + \overline{\Delta Offset} + \overline{\Delta Duration} \quad (1)$$

where $Extra_{IMU}$ represents the number of "extra" movements obtained from the IMU data compared to the number of movements identified by the GS. $Missing_{IMU}$ represents the number of missing movements compared to the number of movements identified by the GS. $Total_{IMU}$ is the total number of movements obtained from the IMU data. $\overline{\Delta Onset}$ and $\overline{\Delta Offset}$ represent the onset and offset mean errors (expressed in seconds) between the movements obtained from IMU data and the GS, respectively. $\overline{\Delta Duration}$ represents the mean duration difference (expressed in seconds) between the movements obtained from IMU data and the GS. The best pair of parameters α and β was determined by finding the minimum value of the cost function Fc.

2.6 PerformanceAssessment

To evaluate the performance of each of the presented methods, several parameters have been used. For each trial, it has been calculated whether the specific method detected erroneous movements (N_{mov}) compared to the GS, the percentage of erroneous movements (Err_{Mov}) with respect to the GS, the onset and offset Mean Absolute Error (MEA_{Onset} and MEA_{Offset}, respectively) against the GS. Notice that MEA_{Onset} and MEA_{Offset}were calculated only for those movements that were consistent between the GS- and the IMU-based segmentation. Additionally, the duration of each movement (T) was calculated as the difference between the offset and onset time instants.

In the following analyses, the average over the three trials of the temporal parameters (i.e., percentage of erroneous movements, onset/offset mean absolute error, and movement duration) was considered.

2.7 Drinking Task Characterization

After the evaluation of the effectiveness of the identification of voluntary movements from the inertial data, the drinking task was characterized in terms of the duration of each sub-phase. First, each repetition of the drinking task was split using the longer resting time (approximately 4 s) between consecutive movements. Then, the single sub-phases were identified and classified using the SP as a reference. For each segmentation method, the mean duration of each sub-phase over trials was calculated as the difference between the offset and onset time instants and compared against the GS.

2.8 Statistical Analysis

We applied the Kolmogorov-Smirnov test to assess the data distribution normality of the percentage of erroneous movements, the onset and offset mean absolute error, and the movement duration. Based on the Kolmogorov-Smirnov test results, a *1-way* ANOVA (in case of normal distributions) or a Kruskal-Wallis test (for non-normal distributions) was used followed by *post-hoc* analysis with Bonferroni adjustments for multiple comparisons. All the analyses were performed setting the significance level (α) at 0.05. Parameter estimates are represented as mean ± standard error over the population. The effect size of the statistically significant differences was calculated through the Hedges' g statistic [26]. A g value of 0.2, 0.5, and 0.8 are considered a small, medium, and large effect size, respectively.

The statistical analyses were performed using the Statistical and Machine Learning Toolbox of MATLAB release r2023b (The MathWorks Inc., Natick, MA, USA).

3. Results and Discussion

3.1 DynAMoS Optimization Process

Figure 4 shows the results of the DynAMos optimization process aimed at selecting the optimal α and β values. The optimal parameters selected were $\alpha = 0.8$ and $\beta = 1.4$. All DynAMoS results described in the following sections were obtained using these optimal parameter values.

3.2 Performance Assessment

The performance of IMU-based segmentation approaches against the stereophotogrammetric system (i.e., gold standard) is represented in **Table 1** with the indication of the statistically significant differences.

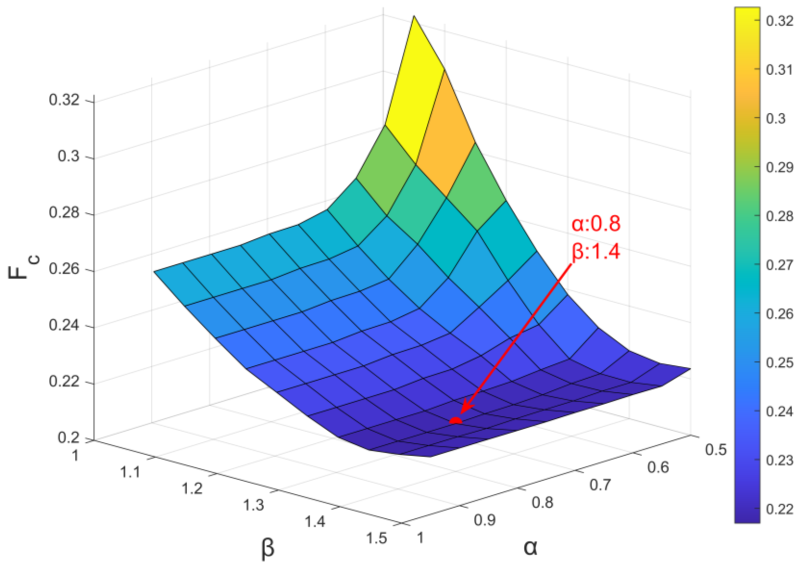

Figure 4. Values assumed by the cost function F_c when considering different α and β. The red dot identifies the minimum of the cost function F_c found when $\alpha = 0.8$ and $\beta = 1.4$.

The SP-based segmentation identified, on average, 100 ± 4 voluntary movements (mean ± standard error) per trial. Considering the IMU-based segmentation approaches, 168 ± 24 movements, 101 ± 7 movements, and 103 ± 5 movements were obtained considering M1, M2, and DynAMoS methods, respectively. Overall, the newly presented algorithm identified only 3% erroneous movements (i.e., 2.8% extra movements and 0.2% missed movements) compared to the GS. M1 resulted in 39.8% erroneous movements (i.e., 39.8% extra movements) compared to the GS, while M2 gave significantly better results, revealing only 3.7% erroneous movements (i.e., 2.5% extra movements and 1.2% missed movements). As shown in **Figure 5**, in some cases, the percentage of missed and extra movements per trial is relatively high, with a maximum of 51.5% and 15.1% of the movements, respectively. Statistically significant differences in the percentage of erroneous movements were detected among all the tested approaches ($p < 0.0001$). In particular, the worst performance was obtained considering the M1 approach. Even if no statistically significant differences in the percentage of erroneous movements were detected between

Table 1. Performance assessment of the three tested approaches against the stereophotogrammetric system.

Performance Assessment	Segmentation Method				Kruskal-Wallis
	GS	**M1**	**M2**	**DynAMoS**	***p*-value**
N_{mov}	$100 \pm 4^{*,\dagger,\ddagger}$	$168 \pm 24^{*,⁑}$	$101 \pm 7^{\dagger,⁑}$	$103 \pm 5^{\ddagger,⁑}$	**< 0.0001**
Err_{Mov} (%)	N/A	$39.8\%^{*,\dagger}$	$3.7\%^{*}$	$3.0\%^{\dagger}$	**< 0.0001**
MAE_{Onset} (s)	N/A	$0.22 \pm 0.05^{*,\dagger}$	$0.10 \pm 0.04^{*,\ddagger}$	$0.07 \pm 0.02^{\dagger,\ddagger}$	**< 0.0001**
MAE_{Offset} (s)	N/A	$0.29 \pm 0.07^{*,\dagger}$	$0.20 \pm 0.04^{*,\ddagger}$	$0.08 \pm 0.03^{\dagger,\ddagger}$	**< 0.0001**
T (s)	$0.97 \pm 0.08^{*}$	$0.98 \pm 0.17^{\dagger}$	$0.67 \pm 0.08^{*,\dagger,\ddagger}$	$0.98 \pm 0.11^{\ddagger}$	**< 0.0001**

Parameters are represented as mean ± standard error over the population.

N/A: Not Applicable; GS: Gold Standard.

Asterisks (*), double asterisks (⁑), daggers (†), and double daggers (‡) represent statistically significant differences between methods.

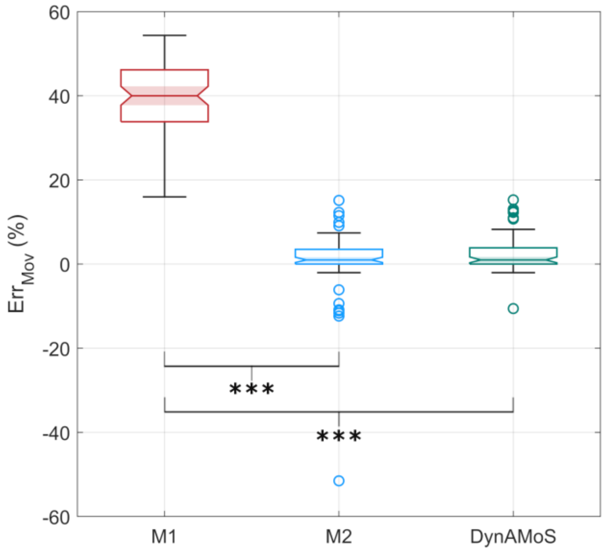

Figure 5. Boxplots representing the percentage of erroneous movements computed between each tested segmentation approach (M1, M2, and DynAMoS) and the gold standard. Statistically significant differences are represented through asterisks (*** p < 0.0001).

M2 and DynAMoS, it is noticeable the difference in the number of outliers (i.e., DynAMoS revealed a reduced number of outliers compared to M2).

These results confirm that the application of a low threshold, as employed by M1, can result in the detection of an excessive number of voluntary movements, which may be attributed to noise or involuntary movements. In contrast, the detection method M2 is characterized by a high number of missing movements, despite the adaptive threshold.

Considering the onset mean absolute errors, statistically significant differences were detected between all the tested approaches ($p < 0.0001$). *Post-hoc* analysis identified significant differences between DynAMoS and M1 ($p < 0.0001$; $g = 3.9$), between DynAMoS and M2 ($p < 0.0001$; $g = 1.3$), and betwen M1 and M2 ($p < 0.0001$; $g = 2.5$). **Figure 6a** represents

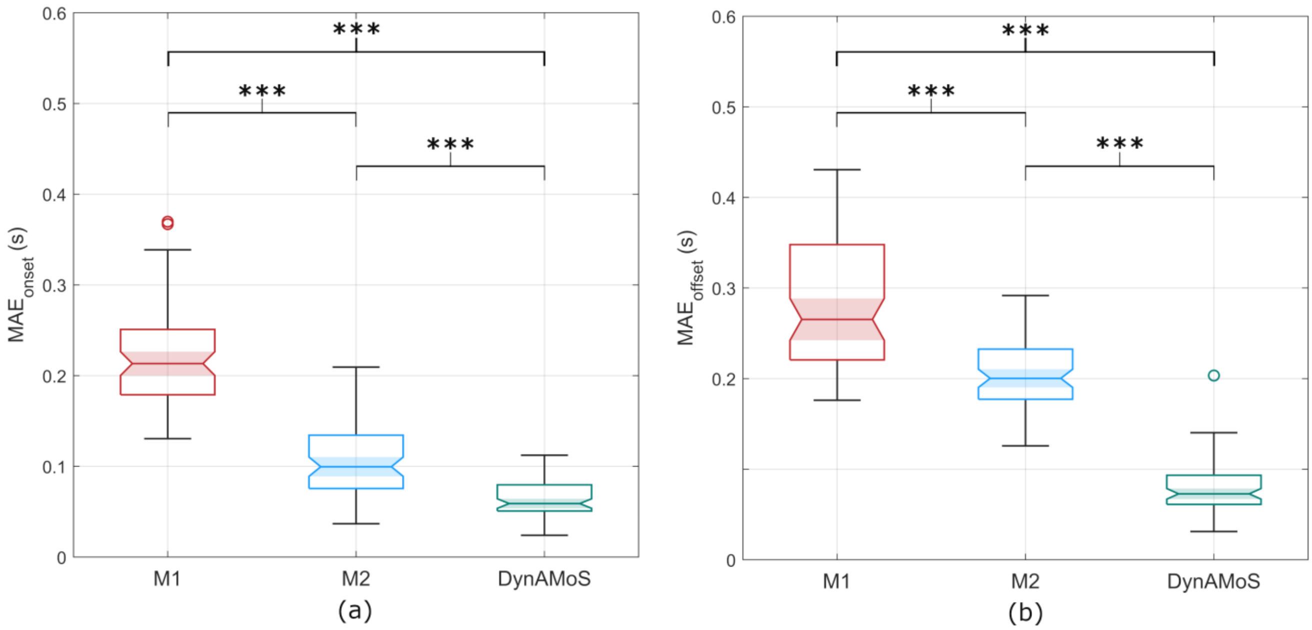

Figure 6. Boxplots representing (a) the MAE_{Onset} and (b) the MAE_{Offset} computed between each tested segmentation approach (M1, M2, and DynAMoS) and the gold standard. Statistically significant differences are represented through asterisks (*** $p <$ 0.0001).

the MAE_{Onset} distributions with the indication of the statistically significant differences. Similarly, when considering the offset mean absolute error, significant differences were detected between DynAMoS and all the tested approaches ($p < 0.0001$). Bonferroni adjustments for multiple comparisons revealed significant differences between DynAMoS and M1 ($p < 0.0001$; $g = 3.7$), between DynAMoS and M2 ($p < 0.0001$; $g = 3.7$), and between M1 and M2 ($p < 0.0001$; $g = 1.4$). **Figure 6b** represents the MAE_{Offset} distributions with the indication of the statistically significant differences. The distributions of the onset and offset mean absolute errors obtained using DynAMoS are largely concentrated below 0.1 s., a value that deviates considerably from those obtained considering M1 (mean absolute error higher than 0.2 s). In contrast, M2 errors have a different behavior. The mean onset error is 0.1 s, with the major part of the distribution lower than 0.15 s, whereas the mean offset error is 0.2 s.

Considering the movement durations, the tested approaches showed statistically significant differences ($p < 0.0001$). In particular, statistically significant differences were detected between M2 and the GS ($p < 0.0001$; $g = 3.6$), between M2 and M1 ($p < 0.0001$; $g = 2.3$), and between M2 and DynAMoS ($p < 0.0001$; $g = 3.3$). The mean duration of the movement, as identified by M2, is approximately 30% shorter than the one identified by the GS. Although there was no statistically significant difference in the mean durations, the distribution obtained applying M1 is notably more variable than the one obtained considering the GS and DynAMoS. A lower and fixed threshold results in longer movements and fast transitions given by small fluctuations around the threshold level, increasing the variability in the results. **Figure 7** shows the distributions of the movement duration for all the tested approaches, with the indication of the statistically significant differences.

3.3 Drinking Task Characterization

Figure 8 and **Table 2** report the drinking task characterization results for all the tested methods.

For all the sub-phases, a statistically significant difference in sub-phase duration was observed. Multiple comparisons resulted in a significant difference between the M1 and

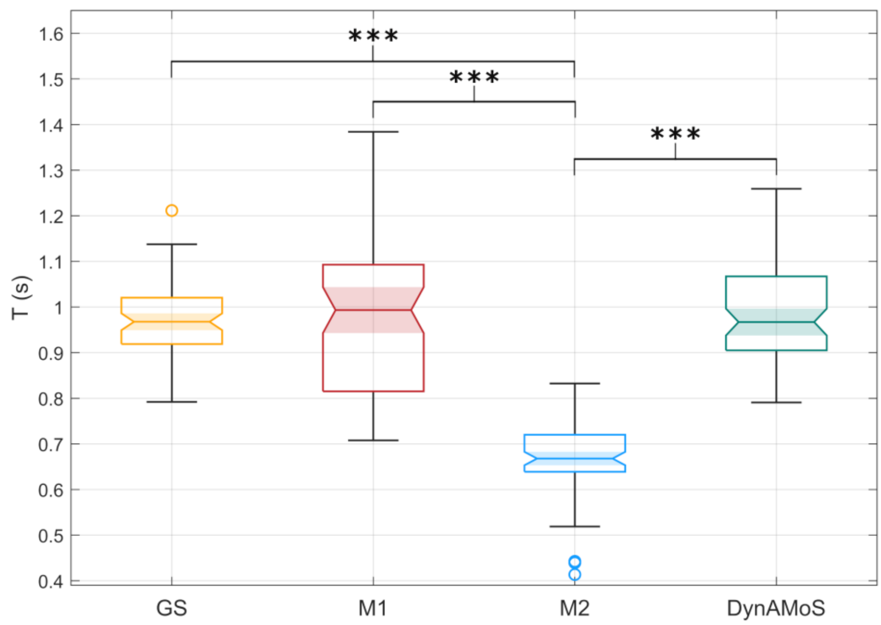

Figure 7. Boxplots representing the movement durations (T) computed considering the GS (yellow), M1 (red), M2 (blue), and DynAMoS (green) methods. Statistically significant differences are represented through asterisks (*** $p < 0.0001$).

Table 2. Drinking task sub-phase durations.

Sub-phase duration (s)	Segmentation Method				Kruskal-Wallis
	GS	**M1**	**M2**	**DynAMoS**	p-value
Phase I	$0.97 \pm 0.11^{*,⁑}$	$1.44 \pm 0.19^{*,\dagger,\ddagger}$	$0.59 \pm 0.14^{⁑,\dagger,\bullet}$	$1.01 \pm 0.14^{\ddagger,\bullet}$	**< 0.0001**
Phase II	$0.98 \pm 0.13^{*,⁑}$	$1.47 \pm 0.17^{*,\dagger,\ddagger}$	$0.79 \pm 0.08^{⁑,\dagger,\bullet}$	$1.02 \pm 0.13^{\ddagger,\bullet}$	**< 0.0001**
Phase III	$0.98 \pm 0.10^{*,⁑}$	$1.44 \pm 0.20^{*,\dagger,\ddagger}$	$0.77 \pm 0.07^{⁑,\dagger,\bullet}$	$1.01 \pm 0.13^{\ddagger,\bullet}$	**< 0.0001**
Phase IV	$0.98 \pm 0.09^{*,⁑}$	$1.54 \pm 0.22^{*,\dagger,\ddagger}$	$0.58 \pm 0.14^{⁑,\dagger,\bullet}$	$1.00 \pm 0.13^{\ddagger,\bullet}$	**< 0.0001**

Parameters are represented as mean ± standard error over the population. GS: Gold Standard.
Asterisks (*), double asterisks (⁑), daggers (†),double daggers (‡), and point (•) represent statistically significant differences between methods.

M2 methods, and between both the M1 and M2 methods and the GS and DynAMoS ($p <$ 0.0001; g > 1.7). In particular, the data distribution obtained considering M2 is below the lower quartile of the other distributions, while the data distribution obtained considering M1 is above the upper quartile of the other distributions. On the other hand, for all the sub-phases, there was no statistically significant difference (p > 0.8) between the timings obtained through the GS and those obtained through DynAMoS. The application of M2 results in a mean duration of the sub-phases that deviates downward from that obtained through the GS of approximately 20%, for Phase II and III, and 40%, for Phase I and IV. It is worth noting that similar sub-phases, in terms of the range of motion but opposed in terms of the goal of the movement, present similar timings and errors. In contrast, the result obtained by applying M1 overestimates movement sub-phase durations by approximately 45%. The estimates obtained by means of DynAMoS align with the GS results.

4. Final Considerations

This study presents a novel segmentation method developed to overcome the limitations of the most popular existing methods published in the literature. In particular, the presented algorithm was compared with the threshold-based segmentation approaches proposed by Schwarz *et al.* [13] (M1) and Carpinella *et al.* [14] (M2).

Although the mean number of movements identified by M2 was the closest to that obtained by the GS, it is worth noticing from the Err_{Mov} distribution represented in **Figure 5** that in numerous instances the number of missing movements was significant. While selecting an adaptive threshold may be more appropriate for different movements, a high threshold can result in a higher percentage of missed movements (51% in the case of the M2 approach), especially when the movement consists of different sub-phases with varying intensities. In contrast, results obtained through the M1 approach indicate a consistent over-detection of voluntary movements, revealing that the threshold is too low and likely influenced by small signal fluctuations close to the threshold (see **Figure 2**). As can be seen from **Figure 5**, DynAMoS Err_{Mov} distribution is similar in variability to the results obtained with M2. However, the number of outliers and the percentage of missed movements are considerably reduced, revealing the reliability of the segmentation.

Focusing on movement onset and offset detection, the method presented in this study was more accurate than the other tested approaches when compared to the GS. In fact, the movement durations of the 4 sub-phases obtained through DynAMoS were closer to the GS (with an average difference of 0.04 s). Previously published research reports that a 15% variation in movement performance metrics is considered a clinically important difference [12]. In our study, movement durations obtained by means of M1 and M2 methods differ from the GS from a minimum of 20% to over 40%, whereas a maximum of 3% variation was obtained considering the newly proposed method. Therefore, the difference in

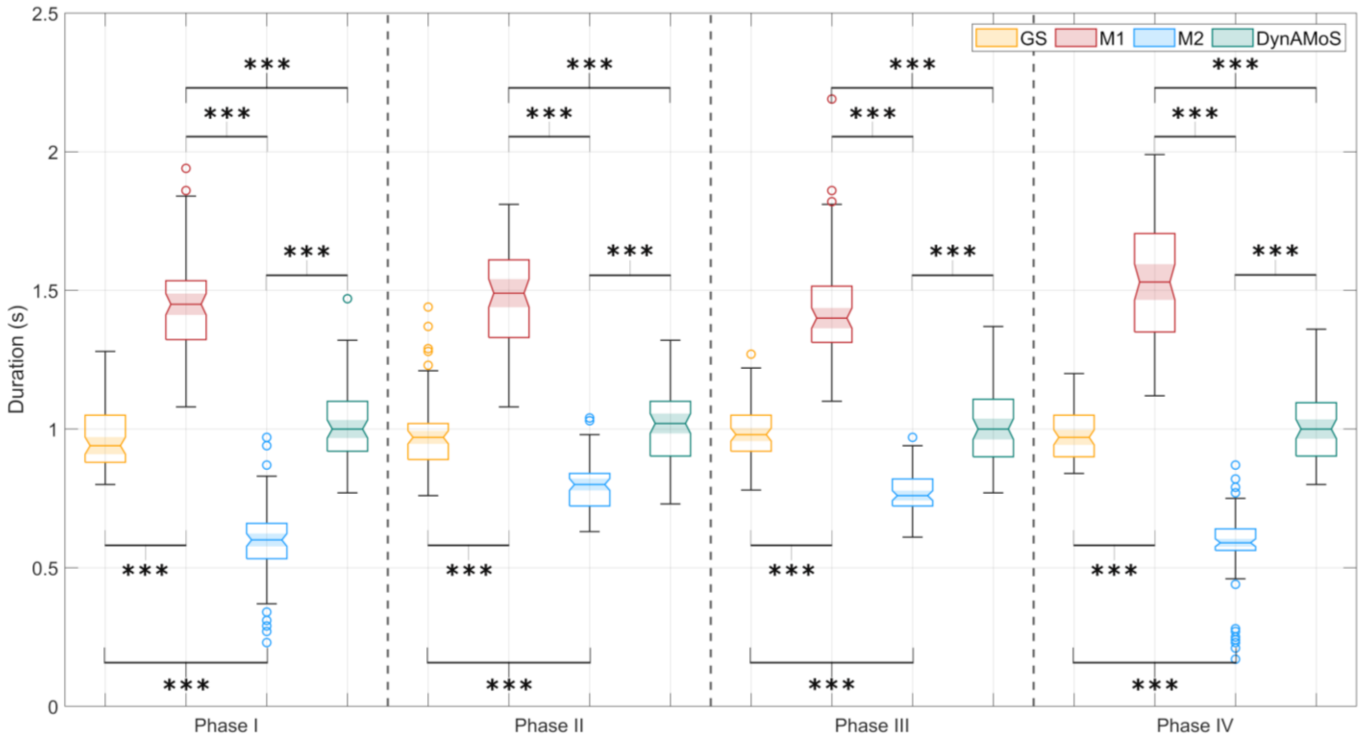

Figure 8. Distribution of the mean duration of the sub-phases of the drinking task for the sample population for the tested methods and the SP Gold Standard. Statistically significant differences are represented through asterisks (*** $p < 0.0001$).

movement timing between the two tested state-of-the-art methods and the GS is considerably higher than 15%, suggesting that the use of these segmentation methods may strongly impact the clinical assessment. In contrast, the small differences in movement timings between DynAMoS and the GS make the proposed method considerably more reliable and potentially applicable in the clinical assessment of patients.

Even though a clinical validation of the method was not performed, it is possible to compare the obtained results with similar results presented in the literature. For example, Patterson *et al.* [27] evaluated post-stroke patients and healthy controls reaching a target at a comfortable speed by using a SP system. On average, the duration of the movements was 0.96 ± 0.27 s and 0.67 ± 0.12 s considering the post-stroke patients and the healthy controls, respectively. The difference in movement durations between the stroke survivors and the healthy controls is lower than the difference in durations observed in our data. Thus, the application of different segmentation approaches may not be able to differentiate between a healthy and a pathological population. Furthermore, Carpinella *et al.* [14] demonstrated a statistically significant difference of approximately 0.4 s in grasp movement duration between Multiple Sclerosis patients and healthy controls. This difference is not substantially larger than the sub-phase duration error between M1, M2, and the GS.

Although the results are promising, there are some limitations associated with the method. The first is the impossibility of applying the algorithm in real-time, due to the adaptive thresholding and the post-processing step. Both these steps require the whole inertial data to compute the required parameters (i.e., the maximum angular velocity norm and the movement duration distribution). Moreover, this study was carried out on healthy subjects only. Further studies are needed to validate this approach for patient assessment in a clinical environment.

5. Conclusions

In this study, we compare a new IMU-based segmentation method for upper limb movements with two popular segmentation methods [13,14]. The movement herein considered is the reach-to-grasp movement, because of its frequent use in the clinical evaluation of patients suffering from upper limb motion disorders. Results show that the proposed method performs significantly better than the two implemented ones. According to Kwakkel *et al.* [12], the segmentation accuracy of DynAMoS could make it available for clinical applications. Using IMU for motion detection and the proposed algorithm for time segmentation of upper limb voluntary movements could make more effective home monitoring applications for assessing the motion improvements of patients following domicile rehabilitation protocols.

Author Contributions: Conceptualization, G.D. and M.G.; methodology, G.D. and M.G.; software, G.D.; validation, G.D. and M.G.; formal analysis, G.D.; data acquisition, G.D. and M.G.; data curation, G.D. and M.G.; visualization, G.D. and M.G.; writing—original draft preparation, G.D., M.K., and M.G.; writing—review and editing, G.D., M.C., D.F., M.K., A.C., and M.G.; supervision, M.G.; project administration, M.K.. All authors have read and agreed to the published version of the manuscript.

Institutional Review Board Statement: The study was conducted in accordance with the Declaration of Helsinki, and approved by the Ethics Committee of Politecnico di Torino (protocol # 24766/2022, approved on July 19, 2022).

Informed Consent Statement: Prior to participation, all participants provided written informed consent.

Data Availability Statement: DynAMoS algorithm, detailed documentation, and a sample dataset are freely available on the BIOLAB GitHub repository (https://github.com/Biolab-PoliTO/DynAMoS).

Conflicts of Interest: The authors declare no conflict of interest.

Acknowledgments: We would like to thank all study volunteers for their participation. Furthermore, thanks go to Dr. David Selkowitz from the MGH Institute of Health Professions for his valuable contribution to the experimental protocol definition.

References

1. Edemekong, P.F.; Bomgaars, D.L.; Sukumaran, S.; Schoo, C. *Activities of Daily Living*; 2024;
2. Amis, A.A. Part 1. Upper Limb Function, Shoulder and Elbow. *Curr. Orthop.* **1990**, *4*, 21–26, doi:10.1016/0268-0890(90)90028-E.
3. Wenning, G.K.; Kiechl, S.; Seppi, K.; Müller, J.; Högl, B.; Saletu, M.; Rungger, G.; Gasperi, A.; Willeit, J.; Poewe, W. Prevalence of Movement Disorders in Men and Women Aged 50-89 Years (Bruneck Study Cohort): A Population-Based Study. *Lancet Neurol.* **2005**, *4*, 815–820, doi:10.1016/S1474-4422(05)70226-X.
4. Knorr, B.; Hughes, R.; Sherrill, D.; Stein, J.; Akay, M.; Bonato, P. Quantitative Measures of Functional Upper Limb Movement in Persons after Stroke. *2nd Int. IEEE EMBS Conf. Neural Eng.* **2005**, *2005*, 252–255, doi:10.1109/CNE.2005.1419604.
5. Alt Murphy, M.; Murphy, S.; Persson, H.C.; Bergström, U.B.; Sunnerhagen, K.S. Kinematic Analysis Using 3D Motion Capture of Drinking Task in People with and without Upper-Extremity Impairments. *J. Vis. Exp.* **2018**, *2018*, doi:10.3791/57228.
6. Pan, B.; Huang, Z.; Jin, T.; Wu, J.; Zhang, Z.; Shen, Y. Motor Function Assessment of Upper Limb in Stroke Patients. *J. Healthc. Eng.* **2021**, *2021*, doi:10.1155/2021/6621950.
7. Aprile, I.; Germanotta, M.; Cruciani, A.; Loreti, S.; Pecchioli, C.; Cecchi, F.; Montesano, A.; Galeri, S.; Diverio, M.; Falsini, C.; et al. Upper Limb Robotic Rehabilitation after Stroke: A Multicenter, Randomized Clinical Trial. *J. Neurol. Phys. Ther.* **2020**, *44*, 3–14, doi:10.1097/NPT.0000000000000295.

8. Ponsiglione, A.M.; Ricciardi, C.; Amato, F.; Cesarelli, M.; Cesarelli, G.; D'addio, G. Statistical Analysis and Kinematic Assessment of Upper Limb Reaching Task in Parkinson's Disease. *Sensors* **2022**, *22*, doi:10.3390/s22051708.
9. Vanmechelen, I.; Haberfehlner, H.; De Vleeschhauwer, J.; Van Wonterghem, E.; Feys, H.; Desloovere, K.; Aerts, J.M.; Monbaliu, E. Assessment of Movement Disorders Using Wearable Sensors during Upper Limb Tasks: A Scoping Review. *Front. Robot. AI* **2023**, *9*, 1–26, doi:10.3389/frobt.2022.1068413.
10. Gu, C.; Lin, W.; He, X.; Zhang, L.; Zhang, M. IMU-Based Motion Capture System for Rehabilitation Applications: A Systematic Review. *Biomim. Intell. Robot.* **2023**, *3*, 100097, doi:10.1016/j.birob.2023.100097.
11. Ostrowska, P.M.; Śliwiński, M.; Studnicki, R.; Hansdorfer-Korzon, R. Telerehabilitation of Post-Stroke Patients as a Therapeutic Solution in the Era of the Covid-19 Pandemic. *Healthc.* **2021**, *9*, doi:10.3390/healthcare9060654.
12. Kwakkel, G.; Van Wegen, E.E.H.; Burridge, J.H.; Winstein, C.J.; van Dokkum, L.E.H.; Alt Murphy, M.; Levin, M.F.; Krakauer, J.W. Standardized Measurement of Quality of Upper Limb Movement after Stroke: Consensus-Based Core Recommendations from the Second Stroke Recovery and Rehabilitation Roundtable. *Int. J. Stroke* **2019**, *14*, 783–791, doi:10.1177/1747493019873519.
13. Schwarz, A.; Bhagubai, M.M.C.; Wolterink, G.; Held, J.P.O.; Luft, A.R.; Veltink, P.H. Assessment of Upper Limb Movement Impairments after Stroke Using Wearable Inertial Sensing. *Sensors (Switzerland)* **2020**, *20*, 1–22, doi:10.3390/s20174770.
14. Carpinella, I.; Cattaneo, D.; Ferrarin, M. Quantitative Assessment of Upper Limb Motor Function in Multiple Sclerosis Using an Instrumented Action Research Arm Test. *J. Neuroeng. Rehabil.* **2014**, *11*, 1–16, doi:10.1186/1743-0003-11-67.
15. Hughes, C.M.L.; Tran, B.; Modan, A.; Zhang, X. Accuracy and Validity of a Single Inertial Measurement Unit-Based System to Determine Upper Limb Kinematics for Medically Underserved Populations. *Front. Bioeng. Biotechnol.* **2022**, *10*, 1–9, doi:10.3389/fbioe.2022.918617.
16. Caruso, M.; Sabatini, A.M.; Laidig, D.; Seel, T.; Knaflitz, M.; Della Croce, U.; Cereatti, A. Analysis of the Accuracy of Ten Algorithms for Orientation Estimation Using Inertial and Magnetic Sensing under Optimal Conditions: One Size Does Not Fit All. *Sensors* **2021**, *21*, 2543, doi:10.3390/s21072543.
17. Repnik, E.; Puh, U.; Goljar, N.; Munih, M.; Mihelj, M. Using Inertial Measurement Units and Electromyography to Quantify Movement during Action Research Arm Test Execution. *Sensors (Switzerland)* **2018**, *18*, 1–23, doi:10.3390/s18092767.
18. Agostini, V.; Aiello, E.; Fortunato, D.; Knaflitz, M.; Gastaldi, L. A Wearable Device to Assess Postural Sway. *2019 IEEE 23rd Int. Symp. Consum. Technol. ISCT 2019* **2019**, 197–200, doi:10.1109/ISCE.2019.8901019.
19. Cereatti, A.; Gurchiek, R.; Mündermann, A.; Fantozzi, S.; Horak, F.; Delp, S.; Aminian, K. ISB Recommendations on the Definition, Estimation, and Reporting of Joint Kinematics in Human Motion Analysis Applications Using Wearable Inertial Measurement Technology. *J. Biomech.* **2024**, *173*, 112225, doi:10.1016/j.jbiomech.2024.112225.
20. Heller, A.; Wade, D.T.; Wood, V.A.; Sunderland, A.; Hewer, R.L.; Ward, E. Arm Function after Stroke: Measurement and Recovery over the First Three Months. *J. Neurol. Neurosurg. Psychiatry* **1987**, *50*, 714–719, doi:10.1136/jnnp.50.6.714.
21. Cappozzo, A.; Cappello, A.; Croce, U.D.; Pensalfini, F. Surface-Marker Cluster Design Criteria for 3-d Bone Movement Reconstruction. *IEEE Trans. Biomed. Eng.* **1997**, *44*, 1165–1174, doi:10.1109/10.649988.
22. Chardonnens, J.; Favre, J.; Aminian, K. An Effortless Procedure to Align the Local Frame of an Inertial Measurement Unit to the Local Frame of Another Motion Capture System. *J. Biomech.* **2012**, *45*, 2297–2300, doi:10.1016/j.jbiomech.2012.06.009.
23. Otsu, N.; Smith, P.L.; Reid, D.B.; Environment, C.; Palo, L.; Alto, P.; Smith, P.L. Otsu 1979 Otsu Method. *IEEE Trans. Syst. Man. Cybern.* **1979**, *C*, 62–66.
24. Xu, X.; Xu, S.; Jin, L.; Song, E. Characteristic Analysis of Otsu Threshold and Its Applications. *Pattern Recognit. Lett.* **2011**, *32*, 956–961, doi:10.1016/j.patrec.2011.01.021.
25. Agostini, V.; Balestra, G.; Knaflitz, M. Segmentation and Classification of Gait Cycles. *IEEE Trans. Neural Syst. Rehabil. Eng.* **2014**, *22*, 946–952, doi:10.1109/TNSRE.2013.2291907.

26. Hedges, L. V. Distribution Theory for Glass's Estimator of Effect Size and Related Estimators. *J. Educ. Stat.* **1981**, *6*, 107–128, doi:10.3102/10769986006002107.
27. Patterson, T.S.; Bishop, M.D.; McGuirk, T.E.; Sethi, A.; Richards, L.G. Reliability of Upper Extremity Kinematics While Performing Different Tasks in Individuals with Stroke. *J. Mot. Behav.* **2011**, *43*, 121–130, doi:10.1080/00222895.2010.548422.